

L10 FePt nanoparticles with distinct perpendicular magnetic anisotropy prepared on Au buffer layers by a micellar method

Y. Gao, X. W. Zhang, Z. G. Yin, F. T. Si, Y. M. Bai et al.

Citation: *J. Appl. Phys.* **109**, 113907 (2011); doi: 10.1063/1.3592972

View online: <http://dx.doi.org/10.1063/1.3592972>

View Table of Contents: <http://jap.aip.org/resource/1/JAPIAU/v109/i11>

Published by the [American Institute of Physics](#).

Related Articles

Mean field theory for a reversibly crosslinked polymer network

J. Chem. Phys. **137**, 024906 (2012)

Controlled growth of epitaxial BiFeO₃ films using self-assembled BiFeO₃-CoFe₂O₄ multiferroic heterostructures as a template

Appl. Phys. Lett. **101**, 022905 (2012)

Ternary eutectic growth of nanostructured thermoelectric Ag-Pb-Te materials

Appl. Phys. Lett. **101**, 023107 (2012)

In situ study of self-assembled GaN nanowires nucleation on Si(111) by plasma-assisted molecular beam epitaxy

Appl. Phys. Lett. **100**, 212107 (2012)

A master-equation approach to simulate kinetic traps during directed self-assembly

J. Chem. Phys. **136**, 184109 (2012)

Additional information on *J. Appl. Phys.*

Journal Homepage: <http://jap.aip.org/>

Journal Information: http://jap.aip.org/about/about_the_journal

Top downloads: http://jap.aip.org/features/most_downloaded

Information for Authors: <http://jap.aip.org/authors>

ADVERTISEMENT



AIP Advances

Special Topic Section:
PHYSICS OF CANCER

Why cancer? Why physics? [View Articles Now](#)

L1₀ FePt nanoparticles with distinct perpendicular magnetic anisotropy prepared on Au buffer layers by a micellar method

Y. Gao,¹ X. W. Zhang,^{1,a)} Z. G. Yin,¹ F. T. Si,¹ Y. M. Bai,¹ X. L. Zhang,¹
S. Qu,^{1,2} and Z. G. Wang¹

¹Key Lab of Semiconductor Materials Science, Institute of Semiconductors, Chinese Academy of Sciences, Beijing, 100083, People's Republic of China

²Eoply New Energy Technology Co. Ltd., Jiangsu 226612, People's Republic of China

(Received 28 January 2011; accepted 18 April 2011; published online 3 June 2011)

FePt nanoparticles were self-assembled on a MgO (001) substrate by a micellar method. We introduced an Au buffer layer to control the lattice orientation and the magnetic alignment of FePt nanoparticles. A distinct *c*-axis preferred orientation of the FePt nanoparticles was achieved during the thermal annealing treatment. The driving force of lattice reorientation is considered to be the result of the stress caused by the lattice misfit between Au and FePt. The degree of *c*-axis orientation is significantly enhanced with increasing Au thickness, which is attributed to the decrease of the in-plane lattice and the improved crystal quality of the Au layer. Perpendicular magnetic anisotropy was observed for the FePt samples with the Au buffer layer. The out-of-plane coercivity and remanence ratio are 3.1 kOe and 0.8, respectively, which far exceed the in-plane values. © 2011 American Institute of Physics. [doi:10.1063/1.3592972]

I. INTRODUCTION

Ordered ferromagnetic nanoparticle arrays have attracted much attention due to their potential applications in ultrahigh density data storage. In such a scheme, a single nanoparticle serves as a magnetic bit, and hence the storage density can be dramatically increased with reduced particle size and interparticle spacing.^{1,2} One major concern since the scheme was put forward is manipulating the direction of the magnetic easy axes.^{3–5} When the magnetic field is applied along the easy axes, the squareness of the hysteresis loop is improved and thus the remanence is close to the saturation magnetization. This is crucial for retaining the maximum magnetic energy for data recording.⁶ From the viewpoint of practical use, the easy axes of magnetic particles should be aligned perpendicular to the sample surface, in order to be compatible with perpendicular recording.⁷ Another key issue for the single-domain recording is to insure the thermal stability of the ferromagnetic nanoparticles. Below a size limit, the nanoparticles will become superparamagnetic rather than ferromagnetic and cannot be used as magnetic media. Face-centered tetragonal (FCT) L1₀ phase FePt, which is composed of alternatingly stacked Fe and Pt layers with easy axes along the [001] direction, possess the largest magnetocrystalline anisotropy constant, K_u (7×10^7 ergs/cc), among the known magnetic materials. This large K_u allows for thermally stable particle diameters down to about 3 nm at room temperature,^{8,9} making FePt nanoparticle an excellent candidate as a data recording media. Therefore, the fabrication of FePt nanoparticle arrays with *c*-axis preferred orientation [consequently, the perpendicular magnetic anisotropy (PMA)] is extremely essential for the realization of ultrahigh density data recording media.

Solution chemical routes, such as colloidal^{10,11} and micellar^{12,13} methods, were proved to be efficient ways to synthesize FePt nanoparticles with uniform size and well-defined interparticle spacing. The as-synthesized nanoparticles are of a face-centered cubic (FCC) structure and are superparamagnetic at room temperature. Although post-annealing favors the FCC-FCT transition, it fails to produce the *c*-axis preferred orientation of the FePt nanoparticles. A tremendous amount of attention has been focused on this issue, while a general strategy is still far from being achieved. Attempts by Gao *et al.* to manipulate the lattice orientation via thermal stress only yielded a slight parallel magnetic anisotropy.¹⁴ Chen *et al.*⁶ have experimented with the possibility of tuning the texture and magnetic alignment via shape-control of the FePt nanoparticles. Again, only parallel magnetic anisotropy was observed. A commonly used route to control the orientation of the magnetic easy axes is to drive the particle rotation by applying an external magnetic field.^{15–17} Using this method, Tamada *et al.*¹⁵ have fabricated a FePt nanoparticles-polystyrene hybrid structure and observed an obvious PMA. However, the distribution of the easy-axis direction estimated from the Mössbauer and the rocking curve measurements is quite wide with a standard deviation of 16.5°. A more uniform distribution of FePt nanoparticles was achieved by the layer-by-layer deposition of polyelectrolyte azobenzene and L1₀ FePt nanoparticles in the magnetic field.¹⁶ However, the rather strong magnetic field (>5 T) employed in those studies greatly increases the fabrication cost and hence, is not suitable for large-scale industrial production. Another possible way to offer the driving force of the *c*-axis orientation is to use the designed stress caused by lattice or thermal misfit between FePt and the selected substrate.¹⁸ Although the lattice mismatch between the FCC MgO substrate and FePt exceeds 8%, attempts to obtain the (001) textured L1₀ nanocomposite FePt-based films have been made by epitaxial growth on a

^{a)}Author to whom correspondence should be addressed. Electronic mail: xwzhang@semi.ac.cn.

MgO (100) substrate using sputtering and molecular-beam epitaxy.¹⁹ However, to our knowledge, there are no reports concerning the fabrication of FePt nanoparticle assemblies with PMA by such a method.

Herein, we introduce an Au buffer layer between the FePt and the MgO (001) substrate to facilitate the growth of [001]-oriented FePt nanoparticles. Indeed, *c*-axis preferred orientation has been observed for samples annealed at 600 °C and above. Magnetic measurements reveal the appearance of a distinct perpendicular anisotropy.

II. EXPERIMENTAL DETAILS

The preparation of FePt nanoparticles is based on the self-assembly of poly(styrene)-poly(4-vinylpyridine), i.e., PS-P4VP, into reverse micelles in toluene. H₂PtCl₆ and FeCl₃ were added into the micellar solution and then the micelles loaded with metal salts were deposited on the Au/MgO (001) substrates by a spin-coating process. The Au buffer layer used here was prepared by radio-frequency (RF) magnetron sputtering with an RF power of 5 W in a pure argon atmosphere of 0.4 Pa. A Pt wetting layer of 2 nm was inserted between Au and the substrate to insure the epitaxial growth of the Au buffer layer. In order to remove the polymer matrix and to reduce the nanoparticles into the metallic state, the as-coated samples were subsequently subjected to an oxygen and hydrogen plasma treatment for 30 min (150 Pa, 100 W) within a homemade RF plasma system. Vacuum annealing treatments were performed to drive the FCC-FCT transformation for FePt nanoparticles. All samples were covered by a 5 nm-thick Au capping layer using RF magnetron sputtering on the top to avoid the oxidation of FePt nanoparticles.

Surface morphologies of the samples were characterized by a NT-MDT Solver P47 atomic force microscope (AFM) in a semi-contact mode. For the x-ray diffraction (XRD) measurements, a Bruker D8 diffractometer with a Cu K α x-ray source was used. Besides the conventional θ - 2θ scans, the rocking curving and azimuthal scans were also performed to determine the crystal quality and the in-plane orientation of the Au buffer layer. Room-temperature magnetic hysteresis loops were measured by a model MicroMag-2900 alternating gradient magnetometer with a saturation field of 18 kOe.

III. RESULTS AND DISCUSSION

Two types of buffer layers, namely Au and Pt, were considered here for the purpose of guiding the texture and magnetic alignment of FePt nanoparticles. Thermodynamically, the stable orientation is determined by the sum of the film surface energy and the film/substrate interfacial energy.²⁰ On the contrary, the growth kinetics also plays an important role in the orientation selection.²¹ The Au layer was deposited directly on the MgO (001) substrates by sputtering under various conditions, however, the expected cubic-on-cubic epitaxial growth of Au (001) on MgO (001) is not observed, and the Au (111) diffraction peak is dominated, as shown in a typical XRD pattern of the Au film/MgO substrate (Fig. 1(a)). Ferrando *et al.*²² have shown that the (001)

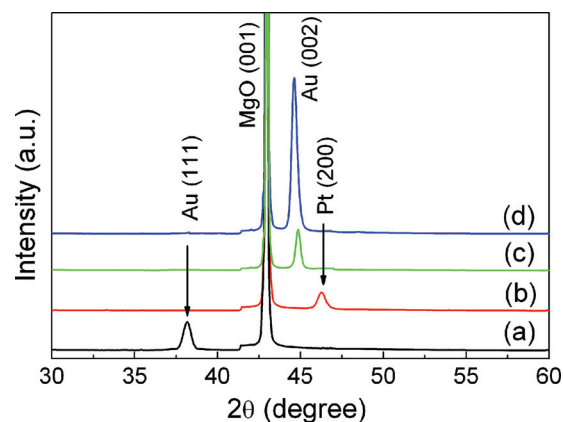


FIG. 1. (Color online) X-ray diffraction patterns of (a) 20 nm Au, (b) 20 nm Pt, and (c) 20 nm Au films with a 2 nm Pt wetting layer and (d) a 50 nm Au film with a 2 nm Pt wetting layer deposited on MgO (001) substrates.

epitaxy is energetically favored only for very small particles (less than 1200 atoms). With increasing particle size, a transition occurs from the [001] to [111] oriented growth of Au on MgO (001). Alternatively, we also attempted the fabrication of a Pt buffer layer on MgO (001) substrates. Fortunately, under a relatively high temperature (~ 400 °C) and a slow deposition rate (< 1 nm/s),²³ the cubic-on-cubic epitaxy of Pt (001) on MgO (001) was realized, as demonstrated in the XRD pattern [Fig. 1(b)]. However, the Pt film is not an ideal candidate as the buffer layer for FePt growth, since the Pt layer may cause a large stoichiometry deviation of FePt nanoparticles from 1:1 and therefore greatly influences the magnetic properties. To facilitate the (001) epitaxy of the Au film on MgO (001) substrates, a 2 nm-thick Pt wetting layer was used in this study. Figures 1(c) and 1(d) show the XRD patterns of 20 and 50 nm Au films with a 2 nm Pt wetting layer deposited on MgO (001) substrates, respectively. Besides the (002) peak, no other Au-related reflections were resolved in the XRD curves, indicating a perfect *c*-axis orientation of the Au films. The Au (002) peak moves toward the small-angle side as the thickness increases due to the strain relaxation. Obviously, the Pt interlayer is indeed beneficial for the [001] oriented growth of the subsequent Au layer.

Figure 2 shows the relevant topography images of the Pt interlayer and Au buffer layer, respectively. The surface of the 2 nm Pt (002) thin film was very smooth and the root-mean-square (RMS) roughness is lower than 0.1 nm, suggesting a two-dimensional growth mode. By contrast, the 40 nm Au film grown on the Pt wetting layer has a coarser surface with a RMS roughness of 1.8 nm. The Au film consists of closely packed square-shaped crystallites. Moreover, the crystallites are well-oriented with their side faces parallel to each other. The strictly parallel side facets of the crystallites are a reflection of the four-fold symmetry of the substrate, implying that the Au film was epitaxially grown on MgO (001).

In order to extract the in-plane orientation of the prepared Au film with respect to the underlying MgO substrate, XRD azimuthal scans (Φ scans) were taken on the out-of-plane {111} reflections of both the Au layer and the MgO

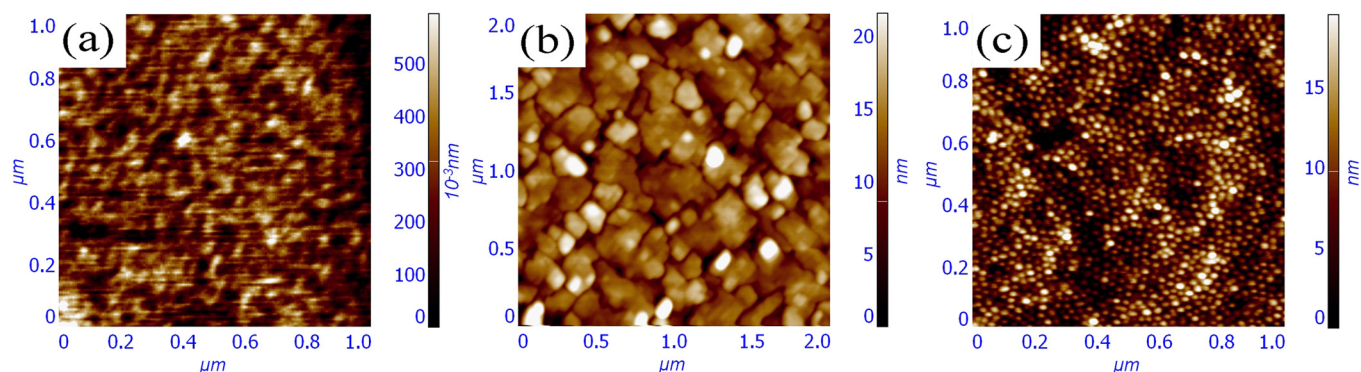


FIG. 2. (Color online) AFM topography images of (a) 2 nm-thick Pt on MgO (001), (b) 40 nm-thick Au layer on Pt/MgO (001), and (c) the as-assembled micelle array on the Au (002) buffer layer.

substrate, as shown in Fig. 3(a). The Φ scan of MgO {111} exhibits four peaks every 90° , revealing the expected four-fold rotational symmetry about the [001] direction. The peaks in the Φ scan of Au {111} have the same symmetry and were detected at essentially identical values of the in-plane rotation angle. This result suggests that the Au film has the cubic-on-cubic orientation with respect to the MgO (001) substrate, and the epitaxial relationship between the Au film and the MgO substrate is determined to be Au(001) [110]||MgO(001)[110]. In addition, the azimuthal angular spread for the Au film decreases with the increasing thickness of Au, and is only 0.8° for the 40 nm-thick Au film. Figure 3(b) also shows the Au (002) rocking curve of the same sample and the full width at half-maximum is found to

be 0.45° . These results indicate an excellent in-plane orientation and good crystal quality of the Au epilayer on the MgO (001) substrate.

FePt nanoparticles were then self-assembled on the Au epilayer. Figure 2(c) illustrates the morphology of the as-synthesized micelles loaded with Fe and Pt salts. The closely packed micelles are uniform in size. The reduced degree of hexagonal order of the micelle array as compared with the previous results^{12,13} may be caused by the rough surface of the Au layer.

A thermal annealing treatment was employed to drive the FCC-FCT transition of the FePt nanoparticles. Figure 4 shows the XRD patterns of the FePt nanoparticles grown on Au buffer layers with various thicknesses (0–40 nm) after annealing at 700°C for 60 min. Note that the small Au (111) peaks located at 38.18° come from the Au capping layer, since they are not resolved in the XRD patterns of pure Au buffer layers, as demonstrated in Fig. 1. It is found that the FePt nanoparticles prepared on a bare MgO (002) substrate present a random orientation, since all the (001), (110), (111), and (200) FePt peaks are clearly visible and comparable in intensity. When an Au (002) buffer layer (10–40 nm) is introduced, the (001) and (002) peaks of the FePt nanoparticles are greatly enhanced, while the reflections from (110) and (111) are significantly weakened. This implies that the

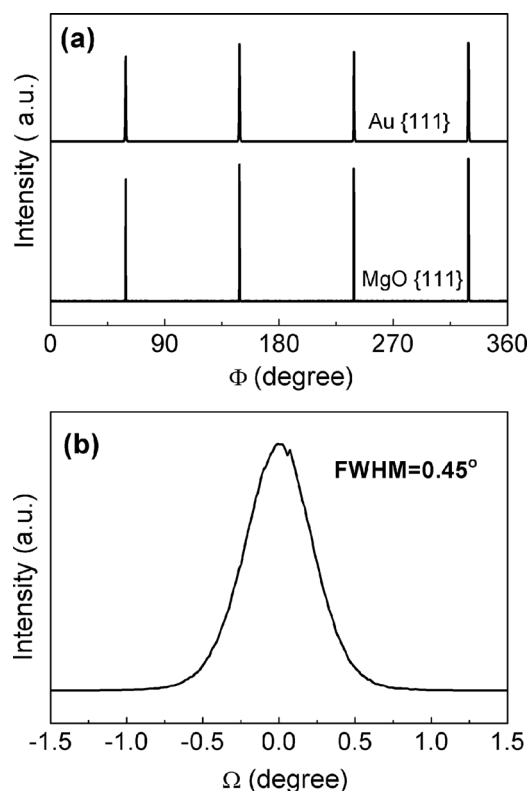


FIG. 3. a) Azimuthal scans of Au {111} and MgO {111} reflections, and (b) the rocking curve of Au (002) for a 40 nm-thick Au layer on Pt/MgO (001).

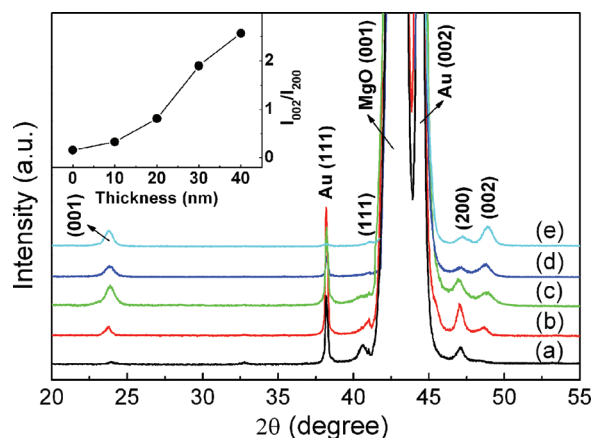


FIG. 4. (Color online) X-ray diffraction patterns of the 700°C annealed FePt nanoparticles on (a) 0 nm, (b) 10 nm, (c) 20 nm, (d) 30 nm, and (e) 40 nm Au (002) buffer layers.

introduction of the Au interlayer is beneficial for the c -axis alignment of the FePt nanoparticles. In addition, the average diameter of these nanoparticles is estimated to be about 10 nm by using Scherer's equation.

Here we note that the annealed FePt nanoparticles are of FCT structure due to the observation of (001) and (110) reflections, as well as the splitting of {002}.¹⁴ The lattice constants, c (3.735 Å), of the FCT FePt is somewhat smaller than the in-plane ones ($a = b = 3.905$ Å).²⁴ At the same time, they are all well below the lattice constant, 4.078 Å, of FCC Au. When the FePt nanoparticles underwent a heat treatment, the Fe and Pt atoms tended to rearrange with the [001] direction of FePt perpendicular to the Au (002) plane. This helps alleviate the stress caused by the lattice mismatch, and therefore reduces the strain energy, finally making the system more thermal stable.²⁵ When the thicknesses of the Au interlayer increases, the intensity ratio I_{002}/I_{200} between the (002) peak and the (200) peak (see the inset of Fig. 4), which is a measure of the degree of c -axis preferred orientation, is significantly enhanced. For instance, the intensity ratio I_{002}/I_{200} increases from 0.4 for the 10 nm Au to 2.3 for the 40 nm Au epilayer. As revealed in Fig. 1, the in-plane lattice constant of Au contracts when the Au interlayer thickness increases, which leads to a better lattice match between Au and FePt. On the other hand, the crystal quality of the Au epilayer is also improved with increasing thickness. Both the decrease of the in-plane lattice constant and the improved crystal quality are beneficial for better c -axis preferred orientation of FePt nanoparticles.

This controlled c -axis preferred orientation leads to a distinct perpendicular magnetic anisotropy. Figure 5 shows the in-plane and out-of-plane hysteresis loops for the FePt nanoparticles with and without a 40 nm-thick Au buffer layer. For the sample without the Au layer, the in-plane and out-of-plane hysteresis loops have similar coercivities and remanence magnetizations, as shown in Fig. 5(a). By

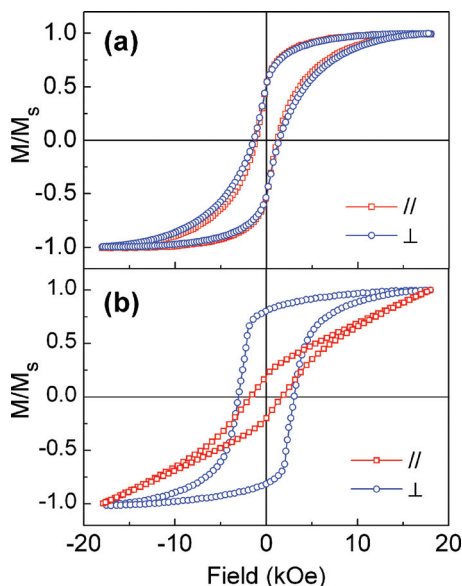


FIG. 5. (Color online) In-plane and out-of-plane M-H loops for the 700 °C annealed FePt nanoparticles (a) without the Au buffer layer and (b) with the 40 nm Au buffer layer.

contrast, the out-of-plane coercivity for the FePt nanoparticles synthesized on Au/MgO (001) is 3.1 kOe, which is much larger than the in-plane coercivity of 1.7 kOe, as revealed in Fig. 5(b). Additionally, with the insertion of the Au buffer layer, both the squareness and the remanence ratio (M_r/M_s) of the out-of-plane loop are greatly enhanced, as compared with those of the in-plane one. The out-of-plane remanence ratio is as large as 0.8, while the in-plane one is only 0.2. These results show that PMA is considerably improved when the Au buffer layer is introduced, consistent with what is concluded from the previously discussed XRD results.

Here we note that the squareness of the out-of-plane loop ($M_r/M_s = 0.8$) is not high enough as compared with the results ($M_r/M_s = 0.92$) obtained by the external field-assistant method.¹⁶ One possible reason is connected to the size distribution of FePt nanoparticles. However, the standard deviation of the size distribution is merely $\sim 6\%$ for FePt nanoparticles,¹⁴ which cannot account for the hysteresis squareness found in Fig. 5. The main reason is believed to be the deviation of the magnetic easy axes of FePt nanoparticles.²⁶ Although the sample, as a whole, has a c -axis preferred orientation, there still exists considerable [100] and [111] oriented FePt nanoparticles, as confirmed by the XRD results in Fig. 4. Except for the squareness, the wider distribution of easy axes can also greatly lower the coercivity. The coercivity, H_C , of 3.1 kOe obtained here (see Fig. 5) is indeed much lower than the theoretically predicted one based on the perpendicular anisotropy constant of 10^7 ergs/cc.²⁷ Multidomain effect may be another possible answer for the lowered H_C . As discussed in our previous work,¹⁴ some of FePt nanoparticles fabricated by the micellar method have twinned domain structures. Other possibilities causing the decreased H_C are stoichiometry deviation and surface oxidation.^{28,29} Recently, we have investigated the composition deviation of FePt nanoparticles from the nominal Fe:Pt molar ratio of the precursors.³⁰ Based on that study, a better control of the nanoparticle stoichiometry has been achieved. Furthermore, the samples were *in situ* transferred into the film deposition chamber during the synthesis process and covered by a 5 nm Au capping layer to avoid oxidation. Therefore, the composition deviation and surface oxidation are not the main causes for the huge decrease of the coercivity, as observed here. As previously discussed, the synthesis of the Au buffer layer with a flatter surface and better crystal quality may facilitate further improvements in PMA. More work is being done in our laboratory and the results will be discussed elsewhere.

IV. CONCLUSIONS

In summary, we have reported the fabrication of FePt nanoparticles with an average size of 10 nm by a micellar method on MgO (001) substrates. The FePt nanoparticles directly synthesized on MgO (001) exhibit a random orientation and no evident magnetic alignment was observed. By contrast, with the introduction of the Au (002) epitaxial layer on MgO (001), distinct c -axis preferred orientation along with the perpendicular magnetic anisotropy of FePt

nanoparticles was obtained. Moreover, the increase of the Au layer thickness was found to facilitate the improvement in PMA. Our method provides a possible new avenue toward ultrahigh density magnetic media.

ACKNOWLEDGMENTS

This work was financially supported by the National Basic Research Program of China (973 Program) under Grant No. 2010CB933800, the National Natural Science Foundation of China under Grant Nos. 51071145 and 61076051, and the Beijing Natural Science Foundation under Grant No. 2102042.

- ¹H. J. Richter, A. Y. Dobin, R. T. Lynch, D. Weller, and R. M. Brockie, *Appl. Phys. Lett.* **88**, 222512 (2006).
- ²C. A. Ross, *Annu. Rev. Mater. Res.* **31**, 203 (2001).
- ³S. S. Kang, J. W. Harrell, and D. E. Nikles, *Nano Lett.* **2**, 1033 (2002).
- ⁴H. Zeng, J. Li, Z. L. Wang, J. P. Liu, and S. H. Sun, *Nano Lett.* **4**, 187 (2004).
- ⁵D. G. Choi, J. R. Jeong, K. Y. Kwon, H. T. Jung, S. C. Shin, and S. M. Yang, *Nanotechnology* **15**, 970 (2004).
- ⁶M. Chen, J. Kim, J. P. Liu, H. Y. Fan, and S. H. Sun, *J. Am. Chem. Soc.* **128**, 7132 (2006).
- ⁷M. Albrecht, G. Hu, I. L. Guhr, T. C. Ulbrich, J. Boneberg, P. Leiderer, and G. Schatz, *Nature Mater.* **4**, 203 (2005).
- ⁸D. Weller and A. Moser, *IEEE Trans. Magn.* **35**, 4423 (1999).
- ⁹H. L. Nguyen, L. E. M. Howard, S. R. Giblin, B. K. Tanner, I. Terry, A. K. Hughes, I. M. Ross, A. Serres, H. Bürckstümmer, and J. S. O. Evans, *J. Mater. Chem.* **15**, 5136 (2005).
- ¹⁰S. H. Sun, C. B. Murray, D. Weller, L. Folks, and A. Moser, *Science* **287**, 1989 (2000).
- ¹¹S. H. Sun, *Adv. Mater.* **18**, 393 (2006).
- ¹²A. Ethirajan, U. Wiedwald, H. G. Boyen, B. Kern, L. Y. Han, A. Klimmer, F. Weigl, G. Kastle, P. Ziemann, K. Fauth, J. Cai, R. J. Behm, A. Romanyuk, P. Oelhafen, P. Walther, J. Biskupek, and U. Kaiser, *Adv. Mater.* **19**, 406 (2007).
- ¹³S. Qu, X. W. Zhang, Z. G. Yin, J. B. You, and N. F. Chen, *Chin. Phys. Lett.* **24**, 3520 (2007).
- ¹⁴Y. Gao, X. W. Zhang, S. Qu, Z. G. Yin, J. B. You, and N. F. Chen, *Nanoscale Res. Lett.* **5**, 1 (2010).
- ¹⁵Y. Tamada, S. Yamamoto, S. Nasu, and T. Ono, *Phys. Rev. B* **78**, 214428 (2008).
- ¹⁶M. Suda and Y. Einaga, *Angew. Chem., Int. Ed.* **48**, 1754 (2009).
- ¹⁷S. S. Kang, Z. Y. Jia, S. F. Shi, D. E. Nikles, and J. W. Harrell, *Appl. Phys. Lett.* **86**, 062503 (2005).
- ¹⁸P. Rasmussen, X. Rui, and J. E. Shield, *Appl. Phys. Lett.* **86**, 191915 (2005).
- ¹⁹H. J. Kim, K. Kim, S. R. Lee, and W. Y. Jeung, *IEEE Trans. Magn.* **44**, 3535 (2008).
- ²⁰P. C. McIntyre, C. J. Maggiore, and M. Nastasi, *Acta Mater.* **45**, 879 (1997).
- ²¹F. Reichel, L. P. H. Jeurgens, E. J. Mittemeijer, *Acta Mater.* **56**, 2897 (2008).
- ²²R. Ferrando, G. Rossi, A. C. Levi, Z. Kuntova, F. Nita, A. Jelea, C. Mottet, G. Barcaro, A. Fortunelli, and J. Goniakowski, *J. Chem. Phys.* **130**, 174702 (2009).
- ²³P. C. McIntyre, C. J. Maggiore, and M. Nastasi, *Acta Mater.* **45**, 869 (1997).
- ²⁴K. H. J. Buschow, P. G. van Engen and R. Jongebreur, *J. Magn. Magn. Mater.* **38**, 1 (1983).
- ²⁵K. E. Waldrip, J. Han, J. J. Figiel, H. Zhou, E. Makarona, and A. V. Nurmikko, *Appl. Phys. Lett.* **78**, 3205 (2001).
- ²⁶W. X. Xia, T. Yamada, K. Tani, J. Numazawa, H. Muraoka, H. Aoi, and Y. Nakamura, *J. Appl. Phys.* **97**, 10N514 (2005).
- ²⁷H. Pfeiffer, *Phys. Status Solidi A* **118**, 295 (1990).
- ²⁸S. Anders, M. F. Toney, T. Thomson, J.-U. Thiele, B. D. Terris, S. H. Sun, and C. B. Murray, *J. Appl. Phys.* **93**, 7343 (2003).
- ²⁹H. B. Wang, M. J. Zhou, F. J. Yang, J. Wang, Y. Jiang, Y. Wang, H. Wang, Q. Li, *Chem. Mater.* **21**, 404 (2009).
- ³⁰S. Qu, X. W. Zhang, Y. Gao, J. B. You, Y. M. Fan, Z. G. Yin, and N. F. Chen, *Nanotechnology* **19**, 135704 (2008).